

Zussmanite in ferruginous metasediments from Southern Central Chile

H.-J. MASSONNE¹, F. HERVÉ², O. MEDENBACH³, V. MUÑOZ² AND A. P. WILLNER³

¹ Institut für Mineralogie und Kristallchemie, Universität Stuttgart, Azenbergstr. 18, D-70174 Stuttgart, Germany

² Departamento de Geología, Universidad de Chile, Casilla 13518, Correo 21, Santiago de Chile, Chile

³ Institut für Mineralogie, Ruhr-Universität, D-44780 Bochum, Germany

ABSTRACT

Zussmanite $\text{KFe}_{13}[\text{AlSi}_{17}\text{O}_{42}](\text{OH})_{14}$, a modulated 2:1 layer silicate, has so far been found only in iron-rich metasediments from Laytonville, California (Agrell *et al.*, 1965). A new occurrence is reported here from Punta Nihue north of Valdivia, Chile, in banded stilpnomelane-schists. These are intercalated in the 'Western Series', a complex of low-grade metamorphic rocks with local high-pressure, low-temperature overprint (e.g. blueschists).

The rock contains conspicuous porphyroblasts of zussmanite of mm size and is composed of chemically distinct bands with the subsequent assemblages: (1) zussmanite–stilpnomelane–quartz, (2) siderite–quartz \pm stilpnomelane (3) apatite–stilpnomelane–quartz \pm siderite. The chemical composition of zussmanite, $(\text{K}_{0.80}\text{Na}_{0.05}\text{Ba}_{0.01})(\text{Fe}_{11.29}^{2+}\text{Mg}_{1.11}\text{Mn}_{0.25}\text{Fe}_{0.14}^{3+}\text{Cr}_{0.01}\text{Al}_{0.19}\text{Ti}_{0.01})[\text{Al}_{1.23}\text{Si}_{16.77}\text{O}_{42}](\text{OH})_{14}$, its optical properties and X-ray data correlate well with the Californian occurrence. Additionally, we present new IR data. In type (2) bands of fine-grained crystals of a K,Al poor mineral formed from siderite and quartz. Its chemical composition is close to that of zussmanite. A similar phase was also reported from Laytonville, California (Muir Wood, 1980).

The rarity of rock-forming zussmanite can be explained by its occurrence in strongly Fe-rich and reduced rocks, as well as, by a possibly narrow P – T stability field.

KEYWORDS: zussmanite, metasediments, schist, Punta Nihue, Chile.

Introduction

THE mineral triplet deerite, howieite, and zussmanite was first discovered by Agrell *et al.* (1965) from the Laytonville quarry, Mendocino County, California. At this locality these hydrated iron-rich silicates occur in meta-ironstones which belong to the blueschist-facies metamorphic rocks of the Franciscan Complex. While deerite and howieite have so far been reported from several localities, typically in blueschist terranes, a second occurrence of zussmanite has not been detected so far. However, a natural occurrence of the Mn analogue of zussmanite, coombsite, was described by Sameshima and Kawachi (1991) in a small lenticular body of Mn-rich siliceous rock of the metasedimentary sequence of the Otago schists, New Zealand.

According to the so far unique natural occurrence, the ideal formula of zussmanite is $\text{K}^{[14]}\text{Fe}_{13}^{[6]}[\text{AlSi}_{17}\text{O}_{42}](\text{OH})_{14}$ (Agrell *et al.*, 1965). Attempts to synthesize the pure end member by high-pressure experiments failed (Lattard and Schreyer, 1981). However, seeded experiments determined the upper temperature stability of zussmanite around 550°C at water pressures above 10 kbar. Zussmanite is a hexagonal phase with a layer structure (Lopes-Vieira and Zussman, 1969). Guggenheim and Eggleton (1987) described it as a modulated 2:1 layer silicate with island-like tetrahedral rings. According to Jefferson (1976), zussmanite shows a layer-stacking disorder that can be explained by the formation of different polytypes. Later on, Muir Wood (1980) reported further types of zussmanite from Laytonville, which are fine-grained. These

types are either richer in manganese or potassium deficient. They were assumed to be late-stage metamorphic products.

With regard to the relatively wide P – T stability of zussmanite (Lattard and Schreyer, 1981) and to the theoretical phase relations calculated by Miyano and Klein (1989) for the system K_2O – FeO – Al_2O_3 – SiO_2 – H_2O , this phase should occasionally occur in nature. Therefore, it was not surprising to discover it again in iron-rich metasediments in Chile. Relatively coarse grained zussmanite was found in a strongly laminated schist. It occurs in mm-thick bands containing stilpnomelane and quartz.

This sample (VM 11) was collected at the Pacific coast between the mouths of Rio Queule and Rio Tolten at the northern edge of Punta Nihue (also written Nigue and Nillhue, S $39^{\circ}17.91'$; W $73^{\circ}13.62'$). Because it is the second occurrence only, our aim was to characterize this zussmanite in detail. Previous information on this zussmanite was given by Massonne *et al.* (1996a) and Muñoz *et al.* (1997).

Geological setting

Similar to paired metamorphic belts, the metamorphic basement within the coastal ranges of Chile south of $34^{\circ}S$ can roughly be divided into a Western Series of low-grade metamorphic rocks locally containing *HP/LT* rocks (e.g. glaucophane schists) and an Eastern Series with intermediate- to high-grade rocks metamorphosed under low-pressure conditions (Gonzalez Bonorino and Aguirre, 1970; Aguirre *et al.*, 1972). Thick clastic sequences with a probable Silurian to Devonian sedimentary age dominate. Metamorphic ages are not older than Carboniferous, becoming younger towards the South in the Western Series and also partly within the Eastern Series (Hervé, 1988).

The low-grade Western Series in the coastal region between 38° and $39^{\circ}30'S$ is interpreted as part of an accretionary prism (Hervé, 1988). Metagreywackes and metapelites dominate. Subordinate are greenschists, which partly show relict pillow structures and have a MORB geochemical signature. Intercalated are lenses of serpentinite, massive Fe–Cu–Zn-sulphides, chromite and 'metacherts' (stilpnomelane-bearing meta-ironstones; spessartine-bearing coticles; Collao *et al.*, 1986). The massive sulphides and metacherts indicate an environment of hydrothermal-exhalative activity before regional meta-

morphism. Rb–Sr-whole rock isochrons yielded ages around 313–331 Ma interpreted as ages of metamorphism, while others around 133–177 Ma are probably due to rejuvenation effects (Hervé *et al.*, 1990). P – T -data for the peak of metamorphism are rare in the area so far. Collao *et al.* (1986) estimated 4.4–9 kbar using sphalerite geobarometry in the system Cu–Fe–Zn–S within the massive sulphides and 5.5 kbar using the mineral chemistry of Na–Ca amphiboles in the greenschists. More recent work on white mica-bearing metapelites and greenschists (Massonne *et al.*, 1996b; Willner *et al.*, 1997) suggests a relatively uniform maximum pressure of 6 to 8 kbar at temperatures around $400^{\circ}C$ within the entire low-grade rock suite. Such conditions already point to low metamorphic geotherms that are indeed typical for an accretionary prism.

Petrography

The zussmanite-bearing schist (VM11), sampled from a metre-thick stilpnomelane-bearing meta-ironstone lense, is strongly foliated and compositionally banded on a mm- to cm-scale. Bands are composed of (1) zussmanite–stilpnomelane–quartz; (2) siderite–quartz \pm stilpnomelane; or (3) apatite–stilpnomelane–quartz \pm siderite. Pure quartz segregations also appear parallel to the banding. Minor pyrite seems to be of secondary origin, at least, concerning strings of less than 1 mm thickness that crosscut the foliation. Pyrite can also be aligned parallel to the foliation in all types of compositional bands. Within the type (1) bands, zussmanite is a major constituent forming abundant conspicuous porphyroblasts of up to 1 mm in size (Fig. 1).

Within a metre distance from the zussmanite-bearing schist, bands with spessartite-rich garnet + stilpnomelane are abundant. Baryte can also occur in the nearby bands. In the vicinity, other lenses with cm-thick green massive zussmanite layers also appear.

The degree of deformation varies strongly. In the zussmanite-bearing bands brown stilpnomelane, that sometimes is also greenish, is mostly strongly aligned parallel to the foliation, as are some zussmanite grains. The foliation is partly due to a crenulation cleavage. Stilpnomelane recrystallised mimetically within microfold hinges. Generally, zussmanite is rotated with strain-free crystallisation of quartz in pressure shadows. Also augen exist with randomly oriented stilpnomelane and strain-free quartz

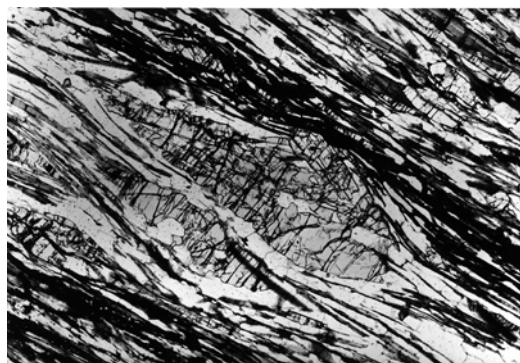


FIG. 1. Zussmanite porphyroblasts in oriented stilpnomelane-quartz bands. Crossed polars. Width of micrograph is 3 mm.

showing a polygonal fabric along preferred long-grain boundaries with stilpnomelane. Zussmanite porphyroblasts often contain inclusions of stilpnomelane, partly oriented quartz and dust of graphite showing relict internal layers.

The strongest deformation and grain-size reduction is observed in some of the siderite-bearing bands, which always show small grain size, also in bands with polygonal fabric. The quartz segregations are coarse grained and display some sutured grain boundaries. The size of the apatite grains in type (3) bands, which are also unoriented, reach 2 mm.

A conspicuous fine-grained mineral occurs in the siderite-bearing bands as small clusters of partly radially grown colourless crystals with birefringence similar to micas. It probably grew during a late stage, at the grain boundaries between siderite and quartz, in particular, replacing siderite. Its appearance resembles the retrograde phase 'ZU2', a zussmanite-type mineral, described by Muir Wood (1980) from zussmanite-bearing rocks in California. It also looks similar to the related minnesotaite found in very low-grade iron-formations elsewhere (e.g. Klein, 1974).

Chemical composition and variability

The chemical compositions of the minerals were determined with the wavelength-dispersive system of an electron microprobe (CAMECA SX50) using an acceleration voltage of 15 kV and a beam current of 10 nA. The beam was defocussed to a diameter of 8 μm . Standards

were topaz for F, jadeite for Na, synthetic pyrope for Mg, Al and Si, synthetic halite for Cl, a K,Ca,Mg,Al-bearing silicate glass for K, a glass of theoretical andradite compositions for Ca and Fe, synthetic TiO_2 for Ti, synthetic Cr_2O_3 for Cr, synthetic spessartite for Mn, synthetic ZnO for Zn and a glass of the bulk composition BaSiO_3 for Ba ($L\alpha$). Counting times for each element were 20 seconds. The PAP matrix correction provided by CAMECA was applied. Semiquantitative analyses were undertaken with the energy dispersive system of the probe. In addition, element distribution maps for Al, Mg and Mn were produced by stepwise scanning with the electron beam over a rectangular area (Bernhardt *et al.*, 1995) using a CAMEBAX.

The large zussmanite crystals turned out to be only slightly inhomogeneous. The average composition (Table 1) is even somewhat closer to the theoretical end-member composition than the type zussmanite from Laytonville (cf. Agrell *et al.*, 1965). Here, some Mn and Mg substitute for Fe. Al is somewhat higher compared to the theoretical formula. This is due to the Tschermak's substitution. A small amount of Na substitutes for K. Fe^{3+} , sometimes appearing in the structural formulae as a minor constituent, was only calculated assuming 31 cations in the tetrahedral and octahedral site and 97 valencies neglecting K+Na. The theoretical amount of 14 OH per formula unit was roughly proven by the oxide sum (Table 1) that is close to 100 wt%. Zussmanite compositions vary somewhat in Mg content. Both analyses given in Table 1 show more or less extreme compositions. According to the distribution maps obtained for a cluster of several zussmanite grains, the rims of this phase are sometimes depleted in Mg.

The stilpnomelane structural formulae were calculated on the basis of 47.375 valencies, neglecting K+Na. Fe^{3+} contents were estimated assuming 15 cations. These contents are very low in spite of the brown colour of stilpnomelane that is often referred to as ferri-stilpnomelane (see Eggleton, 1972). The H_2O content given for stilpnomelane in Table 1 is related here to 6 OH per structural formula (cf. Eggleton, 1972). The resulting oxide sum is then close to 100 wt%. In comparison with the coexisting zussmanite, stilpnomelane shows a higher Mg to Fe^{2+} ratio and is depleted in Mn. The content of trivalent cations in the octahedral site, that is due to the Tschermak's substitution, is also higher in regard of the ratio $\text{Al}^{6l} + \text{Fe}^{3+}$ to sum of octahedral

TABLE 1. Representative mineral analyses from sample VM11. The average is from 70 analyses of zussmanite. For calculation of structural formulae see text. MW = analyses taken from Muir Wood (1980)

	Zussmanite				Stilpnomelane		Zussmanite-type phase	
	10650/37	10650/45	Average	MW	10655/65	10719/7	MW	
SiO ₂	47.82	47.54	47.41	48.42	46.73	51.37	50.19	
TiO ₂	0.03	0	0.02	0	0	0	0	
Al ₂ O ₃	3.29	3.50	3.39	3.78	4.97	0.32	0	
Cr ₂ O ₃	0.06	0.02	0.03	0	0.01	0.01	0	
FeO _{tot}	38.49	37.99	38.63	37.07	35.03	37.14	30.52	
MnO	0.89	0.85	0.83	2.36	0.21	0.16	6.73	
MgO	1.97	2.22	2.09	1.59	3.38	4.21	3.89	
BaO	0.01	0.12	0.05	0	0.20	0.06	0	
Na ₂ O	0.10	0.05	0.07	0	0.73	0.05	0	
K ₂ O	1.70	1.77	1.76	1.90	2.47	0.21	0.16	
F	0.07	0.10	0.07	0	0.14	0	0	
H ₂ O _{calc}	5.92	5.89	5.90	—	5.16	6.09	—	
O=F	-0.03	-0.04	-0.03	—	-0.06	0	—	
Total	100.31	100.00	100.27	95.13	99.18	99.63	91.81	
Si	16.875	16.820	16.768	16.93	8.047	17.697	17.88	
Al ^[4]	1.125	1.180	1.229	1.07	0.953	0.131	0	
Al ^[6]	0.242	0.279	0.183	0.49	0.055	0	0	
Cr	0.017	0.005	0.008	0	0.001	0.004	0	
Ti	0.007	0	0.005	0	0	0	0	
Fe ³⁺	0	0	0.091	0	0.258	0	0	
Fe ²⁺	11.359	11.238	11.335	10.86	4.786	10.699	9.11	
Mn	0.266	0.256	0.250	0.70	0.031	0.046	2.03	
Mg	1.035	1.171	1.103	0.83	0.868	2.160	2.06	
Ba	0.002	0.016	0.007	0	0.014	0.008	0	
Na	0.071	0.035	0.048	0	0.243	0.032	0	
K	0.765	0.801	0.795	0.85	0.543	0.092	0.07	
OH	14	14	14	—	6	14	—	

cations. The chemical variability of stilpnomelane in our sample is surprisingly pronounced. In particular, the Na content is highly variable. The analysis given in Table 1 is close to the average composition.

The late-stage retrograde phase mentioned in the petrographical description is comparable to zussmanite, however, with a marked deficiency of Al and K (Table 1). It also has a somewhat lower Mn content and a slightly higher Mg content compared to zussmanite. The composition is very close to the 'subpotassic zussmanite' described by Muir Wood (1980), which occurs particularly along the rims of zussmanite from the Californian samples (Table 1). By analogy, we believe that we have found the same phase. A calculation of the late retrograde phase as minnesotaite failed.

Optical properties

Because of the limited amount of material available, portions of virtually pure domains of zussmanite were separated from thin-sections, approximately 200 µm thick, under a polarizing microscope by means of a microdrill. Apparatus and procedure are described by Förtsch *et al.* (1992). The majority of the material gained with this method was used for the refinement of the lattice constants.

One optical homogeneous clear crystal was oriented and subsequently measured using a microrefractometer spindle-stage (Medenbach, 1985). The indices of refraction compare well (Table 2) with those determined by Agrell *et al.* (1965) for the chemically slightly different

ZUSSMANITE IN FERRUGINOUS METASEDIMENTS

TABLE 2. Optical properties of zussmanite

	This study	Agrell <i>et al.</i> (1965)
n_o	1.6455(5)	1.645
n_e	1.6253(5)	1.623
Δn	0.020	0.022

zussmanite from the Laytonville quarry, California. The compatibility of physical and chemical data is excellent ($1 - K_p/K_c = 0.024$) according to the categories given by Mandarino (1981). For this calculation, we used the mean zussmanite composition of Table 1 and a calculated density of 3.149 g/cm^3 applying our volume data (see next section).

Powder X-ray diffraction

Several disks of zussmanite obtained with the microdrill were ground in an agate mortar. The powder was spread on a sample holder bearing a single crystal of quartz. The diffraction pattern was obtained with Cu-K α radiation ($\lambda_{K\alpha_1} = 1.54050 \text{ \AA}$) in a Siemens D500. We used 1° slits and a graphite secondary monochromator.

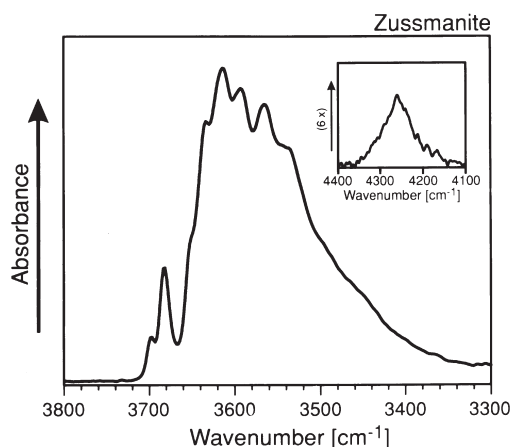


FIG. 2. IR spectra of zussmanite.

Counting times were 4 seconds per 0.01° (2θ) step.

Besides zussmanite, the sample contained some quartz and minor stilpnomelane. We used the quartz as an internal standard, assuming $a = 4.9133, c = 5.4053 \text{ \AA}$. The corrected 2θ values for the zussmanite reflections including their intensity are given in Table 3. The reflections were indexed after calculating the powder pattern with the

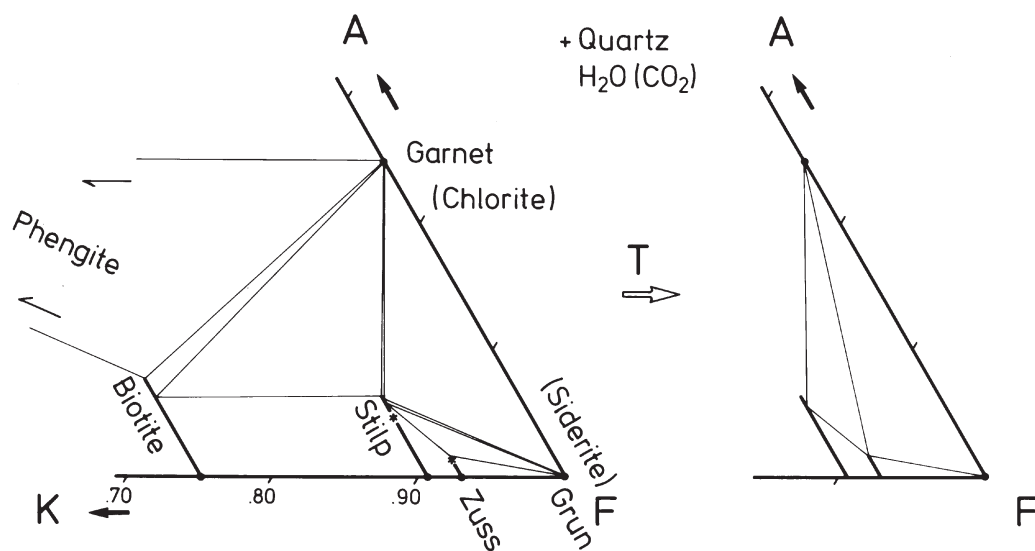


FIG. 3. Tentative phase relations for low-grade metamorphic rocks relevant to the ferruginous portion of a modified A'KF-diagram. Asterisks indicate somewhat simplified stilpnomelane (Stilp) and zussmanite (Zuss) compositions (see Table 1). Grun = grunerite

TABLE 3. Powder X-ray diffraction data ($\lambda_{\text{Cu-K}\alpha_1} = 1.54050 \text{ \AA}$) obtained from a sample with zussmanite, some quartz and minor stilpnomelane. 2θ values in parentheses were weighted half as much as other reflections. For better comparison, I/I_0 of the observed reflections are multiplied by 80 (see $hkl = 315$). n.d. = not determined

hkl	$2\theta_{\text{obs}}$	$2\theta_{\text{calc}}$	$I/I_0 \text{ obs}$	$I/I_0 \text{ calc}$
0 0 3		9.240	n.d.	100
1 0 1		9.283	n.d.	8
1 0 5	17.77	17.768	12	7
2 0 1		17.836		11
0 0 6	18.535	18.541	77	46
2 0 2		18.628		5
1 0 7	23.42	23.408	(24)	12
2 1 1	23.505	23.512	(29)	19
1 1 6	24.055	24.058	37	30
2 1 2		24.126		13
1 0 8	(26.385)	26.354	12	8
0 0 9	27.965	27.967	57	23
2 0 7		28.026		5
1 1 9	31.97	31.978	36	11
2 1 7		32.030		7
3 1 1		32.108		4
3 1 2	32.58	32.572	57	59
2 1 8		34.295		4
3 1 4		34.369		6
3 1 5	35.66	35.665	80	80
0 0 12	37.58	37.591	16	6
3 1 7	38.95	38.937	18	18
3 1 8	40.885	40.868	60	38
3 1 10	45.215	45.226	13	14
3 1 11	47.60	47.621	35	17
3 1 13	52.795	52.784	5	4
3 1 14	55.525	55.535	32	23
4 1 12		56.795		3
5 2 0	56.95	56.944	32	30
0 0 18		57.801		4
5 2 3	(57.82)	57.826	30	19
6 0 6		58.094		4
5 2 6	60.415	60.425	11	10
3 1 16	61.365	61.354	13	15
6 0 9		62.378		3
3 1 17	(64.41)	64.417	4	4
5 2 9	(64.60)	64.616	8	5
6 2 2		67.159		8
6 2 5	69.03	69.028	7	10
5 2 12	70.245	70.254	8	10
3 1 19	70.865	70.852	19	13
6 2 7		71.137		6
6 2 11	(77.345)	77.321	4	6
0 0 24	80.235	80.239	4	2

program LAZY PULVERIX (Yvon *et al.*, 1977) using the structural data of Lopes-Vieira and Zussman (1969). The calculated pattern is given in Table 3 and shows a good correlation with the pattern observed. 28 reflections in the 2θ range 17° to 82° were used to refine the lattice dimensions (Table 4). The data obtained agree well with those given previously (Lopes-Vieira and Zussman, 1969).

Infrared spectroscopy

A zussmanite disk prepared with the microdrill was reduced to small pieces. The fragments were placed on the planar surface of a single crystal of NaCl and investigated with a BRUKER IFS 48 Fourier transmitted infrared spectrometer. The spectra were recorded several times using an IR microscope in transmission mode. The part of the spectrum shown in Fig. 2 was interpreted as follows. The weak peak at 4260 cm^{-1} is due to a combination of bending and stretching of O–H bonds. Several symmetric and asymmetric O–H stretching bands appear in the range between 3700 and 3500 cm^{-1} .

According to the structure refinement by Lopes-Vieira and Zussman (1969), three different positions for hydrogen exist. One of the seven OH groups is related to the K site of the structure. The corresponding OH bond causes the IR bands close to 3700 cm^{-1} . The duplet between 3670 and 3700 cm^{-1} is interpreted to be the result of the occupancy of the site not only by potassium but also by sodium or none atom. The other O–H bands in the range between 3700 and 3500 cm^{-1} , showing clearly higher absorbance than those between 3670 and 3700 cm^{-1} , are related to the two different but altogether six OH groups per

TABLE 4. Lattice dimensions of hexagonal zussmanite ($Z = 3$)

	This study	Lopes-Vieira and Zussman
$a/\text{\AA}$	11.6510	11.66
$\sigma/\text{\AA}$	0.0008	
$c/\text{\AA}$	28.6879	28.69
$\sigma/\text{\AA}$	0.0021	
$V_{\text{cell}}/\text{\AA}^3$	3372.53	
$\sigma/\text{\AA}^3$	0.45	

formula unit linked to octahedral cations. Although the octahedral sites are mainly occupied by Fe^{2+} , more than two O–H bands can be observed in the range 3520 to 3660 cm^{-1} . This is interpreted to be the effect mainly of some Mg substituting for Fe. Thus, the OH groups causing such bands are not only linked to three Fe^{2+} in their vicinity but also to a combination of Fe^{2+} - Fe^{2+} -Mg or other combinations of octahedral cations. This explanation might also include some Al for Si in the tetrahedral sites and thus different combinations of the tetrahedral atoms close to the hydroxyl groups. Under these circumstances, it is not surprising to detect at least six O–H bands in the range 3520 to 3660 cm^{-1} .

Petrogenetic considerations

The most puzzling problem is the extreme rarity of zussmanite in nature, although it forms rock-forming conspicuous crystals in both Laytonville and Punta Nihue localities and is composed of common elements. It represents a phase in the KF(M)ASH system with limited cation substitutions. Its occurrence in Chilean ferruginous metasediments shows striking similarities with its first and so far unique occurrence in California concerning both the rock chemistry and the probable geotectonic setting. This suggests that its appearance is restricted by both a specific rock composition and a relatively narrow stability range.

In the Chilean and Californian rocks, zussmanite occurs in stilpnomelane-bearing assemblages, and in the Californian samples also together with grunerite and garnet. From the relative phase relationships in the system KFASH (Fig. 3) it becomes apparent that at relatively low temperatures, zussmanite forms only in rocks with compositions plotting within very small two- and three-phase fields. These compositions are less aluminous, potassic and more ferruginous than stilpnomelane. According to phase relations appearing in the Californian rocks, a clearly wider compositional space exists (Fig. 3), but these relations might be due to a very narrow temperature range. Moreover, the breakdown of zussmanite to grunerite + biotite at around 550°C (Lattard and Schreyer, 1981) also requires a three-phase field for zussmanite + garnet + biotite after decomposition of stilpnomelane (cf. Muir Wood, 1980). But again, the temperature range for the stability of this assemblage might be very narrow. Furthermore zussmanite rocks seem to be rather

reduced as evidenced by the occurrence of graphite and siderite in such rocks and the low $\text{Fe}^{3+}/\text{Fe}^{2+}$ -ratio in zussmanite itself. Such conditions are not common in the ferruginous protoliths and, thus, might be a further explanation for the rarity of zussmanite (Lattard and Schreyer, 1981).

Acknowledgements

Our thanks are due to H.J. Bernhardt for kindly supporting our microprobe work. K. Röller prepared the IR spectra. Our cooperation project was financially supported by the German Ministry for Research and Technology (BMFT, now BMBF), Billiton Minerals Chile and Cátedra Presidencial to F.H. A previous version of the manuscript was critically reviewed by Jim Chisholm. We thank especially for his comments on IR spectroscopy.

References

- Agrell, S.O., Bown, M.G. and McKie, D. (1965) Deerite, howieite and zussmanite, three new minerals from the Franciscan of the Laytonville district, Mendocino Co., California. *Amer. Mineral.*, **50**, 278.
- Aguirre, L., Hervé, F. and Godoy, E. (1972) Distribution of metamorphic facies in Chile: an outline. *Krystallinikum*, **9**, 7–19.
- Bernhardt, H.J., Massonne, H.-J., Reinecke, T., Reinhardt, J. and Willner, A. (1995) Digital element distribution maps, an aid for petrological investigations. *Ber. Deutsch. Mineral. Ges. Beih. Eur. J. Mineral.*, **7(1)**, 28.
- Collao, S., Kojima, S. and Oyarzun, R. (1986) Geotermobarometria en los sulfuros macizos de la franja metamórfica de esquistos verdes, Chile Central-Sur. *Rev. Geol. Chile*, **28**, 3–16.
- Eggleton, R.A. (1972) The crystal structure of stilpnomelane. Part II. The full cell. *Mineral. Mag.*, **38**, 693–711.
- Förtsch, E., Uhr, W. and Wondraschek, H. (1992) A novel application of the spindle stage. *Microscope*, **40**, 31–6.
- Gonzalez Bonorino, F. and Aguirre, L. (1970) Metamorphism of the crystalline basement of Central Chile. *J. Petrol.*, **12**, 149–75.
- Guggenheim, S. and Eggleton, R.A. (1987) Modulated 2:1 layer silicates: Review, systematics, and predictions. *Amer. Mineral.*, **72**, 724–38.
- Hervé, F. (1988) Late Paleozoic subduction and accretion in Southern Chile. *Episodes*, **11**, 183–8.
- Hervé, F., Pankhurst, R.J., Brook, M., Alfaro, G., Frutos, J., Miller, H., Schira, W. and Amstutz, G.C. (1990) Rb-Sr and Sm-Nd data from some massive sulfide

- occurrences in the metamorphic basement of south-central Chile. In *Stratabound Ore Deposits in the Andes* (L. Fontbote, G.C. Amstutz, M. Cardozo, E. Cedillo and J. Frutos, eds.) 221–8, Springer-Verlag, Berlin, Heidelberg.
- Jefferson D.A. (1976) Stacking disorder and polytypism in zussmanite. *Amer. Mineral.*, **61**, 470–83.
- Klein, C. (1974) Greenalite, stilpnomelane, minnesotaite, crocidolite and carbonates in a very low-grade metamorphic Precambrian iron-formation. *Canad. Mineral.*, **12**, 475–98.
- Lattard, D. and Schreyer, W. (1981) Experimental results bearing on the stability of the blueschist-facies minerals deerite, howieite, and zussmanite, and their petrological significance. *Bull. Mineral.*, **104**, 431–40.
- Lopes-Vieira, A. and Zussman, J. (1969) Further detail on the crystal structure of zussmanite. *Mineral. Mag.*, **37**, 49–60.
- Mandarino, J.A. (1981) The Gladstone-Dale relationship: Part IV. The compatibility concept and its application. *Canad. Mineral.*, **19**, 441–50.
- Massonne, H.-J., Willner, A.P., Hervé, F. and Muñoz, V. (1996a) Zussmanit und ein Zussmanit-ähnliches Mineral in Fe-reichen Metasedimenten aus dem südlichen Zentralchile. *Ber. Deutsch. Mineral. Ges., Beih. Eur. J. Mineral.*, **8(7)**, 183.
- Massonne, H.-J., Hervé, F., Muñoz, V. and Willner, A.P. (1996b) New petrological results on high-pressure, low-temperature metamorphism of the Upper Palaeozoic basement of Central Chile. *Troisième Symp. Int. sur la Géodynamique Andine, Saint-Malo (France)*, Ext. Abstr., 783–5.
- Medenbach, O. (1985) A new microrefractometer spindle-stage and its application. *Fortschr. Mineral.*, **63**, 111–33.
- Miyano, T. and Klein, C. (1989) Phase equilibria in the system $K_2O-FeO-MgO-Al_2O_3-SiO_2-H_2O-CO_2$ and the stability limit of stilpnomelane in metamorphosed Precambrian iron-formations. *Contrib. Mineral. Petrol.*, **102**, 478–91.
- Muir Wood, R. (1980) The iron-rich blueschist-facies minerals: 3. Zussmanite and related minerals. *Mineral. Mag.*, **43**, 605–14.
- Muñoz, V., Hervé, F., Massonne, H.-J., Medenbach, O. and Willner A.P. (1997) Primer hallazgo de zussmanita en Chile, indicador de facies metamórficas de alta presión-baja temperatura. *Actas VIII Congr. Geol. Chileno Antofagasta*, 237–41.
- Sameshima, T. and Kawachi, Y. (1991) Coombsite, Mn analogue of zussmanite, and associated Mn-silicates, parsettensite and caryopilite, from southeast Otago, New Zealand. *N.Z. J. Geol. Geophys.*, **34**, 329–35.
- Willner, A.P., Massonne, H.-J. and Hervé, F. (1997) Wide-spread high pressure/low temperature-metamorphism of the Upper Palaeozoic basement of Central and Southern Chile. *Abstr. suppl. 1, Terra Nova* **9**, EUG 9, 327.
- Yvon, K., Jeitschko, W. and Parthe, E. (1977) LAZY PULVERIX, a computer program, for calculating X-ray and neutron diffraction powder patterns. *J. Appl. Crystallogr.*, **10**, 73–4.

[Manuscript received 4 September 1996:
revised 19 February 1998]